Molecular Structure and Interactions in the Ionic Liquid 1-Ethyl-3-methylimidazolium Bis(Trifluoromethylsulfonyl)Imide.

ARTICLE *in* THE JOURNAL OF PHYSICAL CHEMISTRY A · MARCH 2014

Impact Factor: 2.69 · DOI: 10.1021/jp502124y · Source: PubMed

THE JOURNAL OF PHYSICAL CHEMISTRY A

Article

pubs.acs.org/JPCA

Molecular Structure and Interactions in the Ionic Liquid 1-Ethyl-3-methylimidazolium Bis(Trifluoromethylsulfonyl)imide

Nilesh R. Dhumal,[†] Kristina Noack,[‡] Johannes Kiefer,[‡,§,¶] and Hyung J. Kim*[,†,∥]

[†]Department of Chemistry, Carnegie Mellon University, Pittsburgh, Pennsylvania 15213, United States

[‡]Lehrstuhl fuer Technische Thermodynamik and Erlangen Graduate School in Advanced Optical Technologies, University Erlangen-Nuremberg, D-91058 Erlangen, Germany

[§]School of Engineering, University of Aberdeen, Aberdeen AB24 3UE, United Kingdom

[∥]School of Computational Sciences, Korea Institute for Advanced Study, Seoul 130-722, Korea

Supporting Information

ABSTRACT: Electronic structure theory (density functional and Møller−Plesset perturbation theory) and vibrational spectroscopy (FT-IR and Raman) are employed to study molecular interactions in the room-temperature ionic liquid 1-ethyl-3-methylimidazolium bis(trifluoromethylsulfonyl)imide. Different conformers of a cation−anion pair based on their molecular interactions are simulated in the gas phase and in a dielectric continuum solvent environment. Although the ordering of conformers in energy varies with theoretical methods, their predictions for three lowest energy conformers in the gas phase are similar. Strong C−H---N interactions between the acidic hydrogen atom of the cation imidazole ring and the nitrogen atom of the anion are predicted for either the lowest or second lowest energy conformer. In a continuum solvent, different theoretical methods yield the same ion-pair conformation for the lowest energy state. In both phases, the density functional method predicts that the anion is in a trans conformation in the lowest energy ion pair state. The theoretical results are compared with experimental observations from Raman scattering and IR absorption spectroscopies and manifestations of the molecular interactions in the vibrational spectra are discussed. The directions of the frequency shifts of the characteristic vibrations relative to the free anion and cation are explained by calculating the difference electron density coupled with electron density topography.

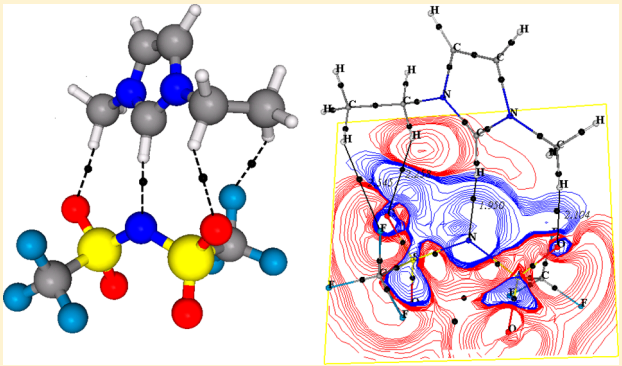

1. INTRODUCTION

Pure ionic materials consisting of bulky and asymmetric organic cations paired with a variety of different anions, often referred to as room-temperature ionic liquids (RTILs), are usually characterized by low melting points, nonvolatility, nonflammability, and good thermal and chemical stability, particularly in the presence of air and moisture.[1−6] RTILs also offer high ionic conductivity and a large electrochemical window, which explain their extensive study for use in, for example, electrochemical devices.[7]

The diversity of differing cation−anion combinations is the basis of the tunability of RTILs' unique properties, thereby leading to a large number of applications in chemistry and related fields.[8] Among many different anionic species, inorganic perfluorinated sulfonylimide anions are of great interest because they are used to produce hydrolytically stable, "hydrophobic" RTILs with relatively low viscosity and high electrical conductivity.[9,10] In particular, bis(trifluoromethylsulfonyl)imide (Tf_2N) exhibits interesting behaviors due to diffuse charge distribution. The delocalized negative charge along the S−N−S core in Tf_2N allows, for instance, the formation of low melting, fluid ionic liquids when paired with a broad range of counterions including ammonium, pyridinium, imidazolium, and pyrrolidinium cations.[11,12] As such, Tf_2N is one of the most widely studied anions in this anionic class.

From the first principles perspective, it is the molecular interactions between cations and anions and the interplay between the short-range and long-range interactions that govern the details of RTILs' physicochemical properties, e.g., a low lattice energy and thus a low melting point.[13−22] Therefore, proper understanding of interionic interactions, including specific hydrogen bonding interactions and nonspecific solvation effects, is important to enable a task-specific design, synthesis, and optimization of ionic compounds that are liquid at room temperature.[9−11] Analysis of electronic structure via molecular orbital methods can shed illuminating light on molecular interactions in ionic liquids.

In recent years Raman and infrared spectroscopy has been widely used to study the molecular interactions in ionic liquids.

Received: March 6, 2014
Published: March 10, 2014

   dx.doi.org/10.1021/jp502124y | J. Phys. Chem. A 2014, 118, 2547−2557

Berg[23] and co-workers used Raman spectroscopy coupled with ab initio calculations to investigate the hydrogen bonding interactions in RTILs based on 1-alkyl-3-methylimidazolium cations (cf. Figure 1). In the case of the Tf_2N anion

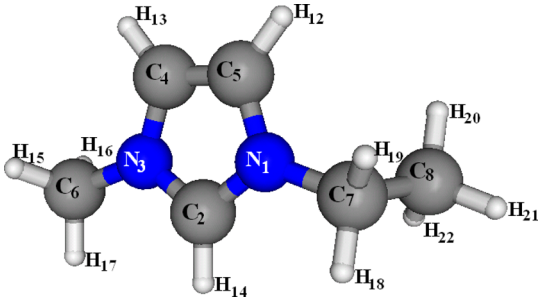

Figure 1. Molecular structure of the 1-ethyl-3-methylimidazolium ion and its atomic numbering scheme.

conformation in 1-alkyl-3-methylimidazolium RTILs, it was found that the trans conformation is favored over the cis.[24,25] The temperature dependence of its conformational changes has also been examined experimentally by Lassègues et al.[26] and Koddermann.[27] Tsuzuki et al.[28] have noted in their ab initio study that the magnitude and directionality of ion pair interactions are important to the dissociation and association behaviors of the ions in RTILs. All these studies share a common view that the molecular interactions in ionic liquids are of great importance and require further investigation.

In this article, we present a detailed analysis of molecular interactions and conformational states of 1-ethyl-3-methylimidazolium bis(trifluoromethylsulfonyl)imide ([EMIm][Tf_2N]) (Figures 1 and 2) via the ab initio methods at the density functional theory (DFT) and second-order Møller–Plesset perturbation theory (MP2) levels, and via experimental Raman and FT-IR spectroscopy. Compared to our previous study on 1-ethyl-3-methylimidazolium acetate and 1-ethyl-3-methylimidazolium ethyl sulfate ion pairs,[29,30] one important extension is the inclusion of solvation effects using the self-consistent reaction field (SCRF) method.[31,32] According to many experimental and simulation studies, the effective polarity of RTILs measured as solvatochromic shifts is comparable to that of highly polar solvents.[33] We therefore model the [EMIm]-[Tf_2N] medium as a dielectric continuum environment and study solvation effects on ion pair conformations and vibrational dynamics. Different conformers are simulated on the basis of different molecular interactions of the [EMIm]-[Tf_2N] ion pair in the gas phase and in solution. The strength of the molecular interactions is analyzed employing electron density topography. The DFT results for molecular vibrations are related to interionic interactions and compared with the experimental data. Frequency shifts in different directions are further analyzed via the difference electron density coupled with electron density topography.

The outline of this paper is as follows. In section 2, the computational and experimental methods used in this work are described briefly. The results and their discussions are presented in section 3. Section 4 concludes.

2. MATERIALS AND METHODS

2.1. Computational Method. We employed computational protocols similar to those of our prior studies.[29,30] Briefly, restricted Hartree–Fock (HF) self-consistent molecular orbital

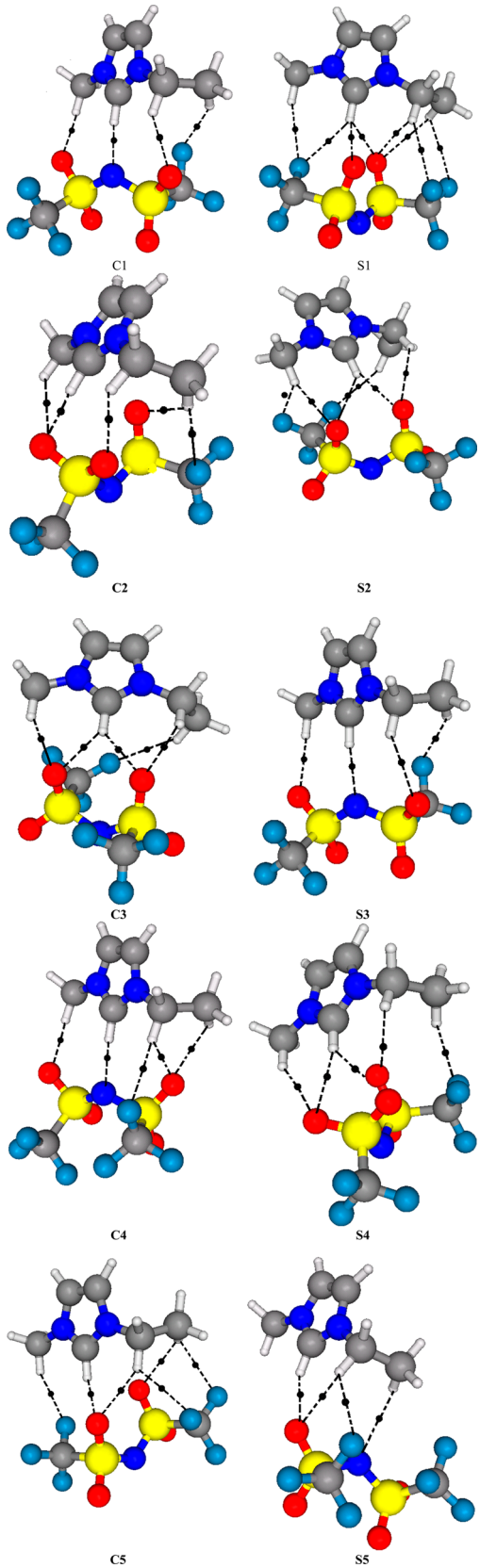

Figure 2. Optimized geometries of the different conformers of 1-ethyl-3-methylimidazolium bis(trifluoromethylsulfonyl)imide. Results in the gas phase (**C**) and in the dielectric continuum (**S**) are shown on the left and right, respectively. Filled circles in black show the bond critical points. See text for details.

dx.doi.org/10.1021/jp502124y | J. Phys. Chem. A 2014, 118, 2547–2557

Table 1. Relative Stabilization Energies (kJ mol^{-1}) of Different Conformers of 1-Ethyl-3-methylimidazolium Bis(trifluoromethylsulfonyl)imide in the Gas Phase and in the Dielectric Continuum Environment with ε = 38

	gas phase				solution		
conformer	B3LYP	MP2	B97D	conformer	B3LYP	MP2	B97D
C1	0.0	4.72	1.8	**S1**	0.0	0.0	0.0
C2	1.0	0.0	4.8	**S2**	0.9	0.97	2.6
C3	2.7	7.54	0.0	**S3**	1.4	2.60	4.1
C4	4.1	8.85	7.3	**S4**	11.2	9.51	13.6
C5	7.5	12.42	6.2	**S5**	11.5	1.85	1.9

calculations were performed on different conformers of the ion pair using the GAUSSIAN 03 program[34] with the internally stored 6-31G(d,p) basis set. Geometry optimization was examined with different methods, viz., the density functional theory with the hybrid B3LYP functional[35,36] and with Grimme's B97D functional including dispersion,[37] and the MP2 perturbation theory. Normal vibrations were assigned by visualizing displacements of atoms around their equilibrium (mean) positions using the UNIVIS-2000 code.[38]

The molecular electron density topography was computed and critical points were identified.[39] Four different types of nondegenerate critical points of rank 3 were considered. These include: maxima (3, 3), e.g., nuclear positions, minima (3, −3) generally known as cage critical points and two types of saddle points, and (3, −1) and (3, +1), respectively, referred to as the bond critical and ring critical points. Here R and σ of (R, σ) represent, respectively, the number and algebraic sum of eigenvalues of the Hessian matrix. The difference electron density ($\Delta\rho$) was calculated by subtracting the sum of electron densities of the isolated cation and anion from the electron density of [EMIm][Tf_2N] complexes. For the isolated cation and anion, the same geometries as in the conformer were used in the calculations of $\Delta\rho$.

The SCRF calculations[31,32] were performed in the B3LYP/6-31G**, B97D/6-31G**, and MP2/6-31G** framework using the polarizable continuum model (PCM) implemented in the Gaussian program. Electrostatic interactions of the ion pair with surrounding ions were effectively accounted for by introducing apparent dielectric constant ε for the RTIL environment. We note that this approach, originally introduced for quadrupolar solvents, such as benzene and supercritical carbon dioxide, was able to describe solvation effects in nondipolar solvents.[40−42] In the present study, we employed ε = 38 to model [EMIm]-[Tf_2N] in the PCM framework. The use of this ε value is based on MD simulation results[43−45] that imidazolium-based ILs show somewhat larger solvatochromic shifts and therefore are effectively more polar than acetonitrile even though their dielectric constant is considerably lower than the acetonitrile value (ε = 36).

2.2. Experimental Methods. *Chemicals.* The synthesis of 1-ethyl-3-methylimidazolium bis(trifluoromethylsulfonyl)imide has been described in a previous paper.[46]

Raman Spectroscopy. Two sets of Raman spectra were recorded using different setups. The conventional Raman spectrum was recorded with a spectral resolution of about 8 cm^{-1} employing a continuous-wave frequency-doubled Nd:YAG laser at 532 nm. Elastically scattered light was blocked by an OG550 color glass filter. In addition, polarization resolved Raman spectra in the fingerprint region were recorded with a spectral resolution of 2−3 cm^{-1} using a grating stabilized diode laser at 785 nm. The signal generated in the RTIL sample inside a fused silica cuvette was collected and collimated using an achromatic lens. Elastically scattered light was blocked by a long-pass filter (790 nm cutoff wavelength). The collimated signal then entered a polarizing beam splitter cube and the vertically and horizontally polarized signal components were each focused into an optical fiber that guided the light into two identical spectrometers. The benefits of performing polarization resolved detection are (1) the depolarization ratio can be determined and (2) Raman peaks that result from superposition of symmetric and antisymmetric vibrations can be decomposed and analyzed more easily (for example, concerning the identification and assignment of shoulder bands). For the sake of completeness we note that Raman and IR spectra of [EMIm][Tf_2N] have been discussed in previous work (see refs 46 and 47). The Raman data discussed in the present work, however, allows a more detailed analysis and better comparison with computational results because of the higher spectral resolution and the significantly improved setup for polarization-resolved measurements.

FTIR Spectroscopy. The IR spectrum from 500 to 4000 cm^{-1} was obtained with a Nicolet Model 360 FTIR at 2 cm^{-1} nominal resolution using an ATR module (diamond crystal, one reflection).

3. RESULTS AND DISCUSSION

3.1. Geometric Analysis. We begin by considering stable ion pair conformations in the gas phase, **C1**−**C5**, of which relative stabilization energies and optimized geometries in the B3LYP, B97D, and MP2 theories are presented in Table 1 and Figure 2. For convenience, the atomic numbering scheme employed in the present work is displayed in Figure 1. To avoid any confusion, we mention at the outset that for a given overall ion-pair conformation, e.g., **C1**, both the detailed geometric parameters, such as bond lengths and angles, and relative energy vary with the methods used for calculations. Thus, **C1** is the lowest energy conformer in vacuo in the B3LYP theory, whereas it is predicted to be the second lowest in energy in both the MP2 and B97D frameworks. The lowest energy conformations predicted by the latter two methods are, respectively, **C2** and **C3**. It is worth noting that all three methods predict **C1**−**C3** as the three lowest energy states although their ordering in energy differs. We also notice that compared to B3LYP, **C3** and **C5** states become stabilized relative to **C1** by 3−5 kJ mol^{-1} in the B97D theory. This is attributed to the dispersion effect explicitly included in B97D.

The Tf_2N anion in the **C1**, **C3**, and **C5** states was found to adopt a trans conformation for its C−S−S−C dihedral, whereas a cis conformation was predicted for **C2** and **C4**. The ion pair in **C1** and **C4** conformations exhibits C−H···N interion interactions through the C_2−H_{14} cation bond. Thus only the B3LYP method yields the presence of the C−H···N interaction in the lowest-energy conformer. Bifurcated C_2−H_{14}···O interactions are present in **C3**, whereas for **C4** and **C5**, the

dx.doi.org/10.1021/jp502124y | J. Phys. Chem. A 2014, 118, 2547−2557

C_7-H_{19} cation bond shows bifurcated interactions with oxygen and fluorine atoms of the anion.

Before we proceed any further, we briefly compare the predictions of the B3LYP, MP2, and B97D methods for two key vibrations, viz., C_2-H_{14} stretching vibration of the cation and SN stretching vibration of the anion, with the experimental results. We note that the intensive Raman structure around 2950 cm^{-1} in Figure 3 is attributed to C_2-H_{14} vibrations,

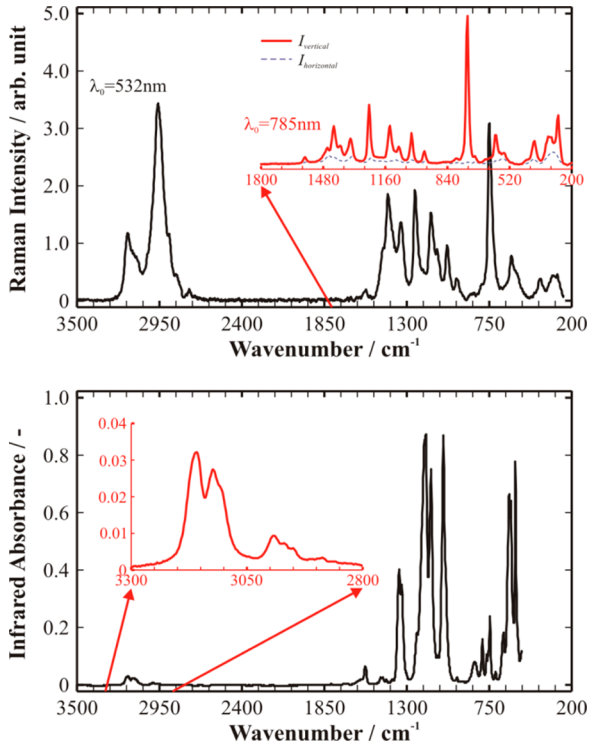

Figure 3. Experimental vibrational spectra: Raman (upper diagram) and infrared spectrum (lower diagram). In the Raman diagram, the inset shows the polarization resolved spectra of the fingerprint region. The inset in the IR diagram displays the enlarged CH stretching region.

whereas the pronounced structure near 740 cm^{-1} is assigned to SN vibrations. The theoretical predictions for the C_2-H_{14} stretching vibration frequencies for two lowest energy conformers are (2931 cm^{-1}, 3155 cm^{-1}), (3155 cm^{-1}, 3073 cm^{-1}), and (3047 cm^{-1}, 2855 cm^{-1}) in the B3LYP, MP2, and B97D methods, respectively (Table 3 and Table S1 of Supporting Information). Here the first and second numbers in the parentheses are the results for, respectively, the lowest and second lowest energy states of the ion pair complex. Except for the MP2 case, the energy difference of the two lowest states is smaller than the thermal energy (Table 1). Thus the second lowest state will have a significant population under ambient conditions in both B3LYP and B97D frameworks. Due to the absence of C_2-H_{14}---N interactions in the lowest energy conformers in MP2 and B97D theories, their C_2-H vibration frequencies, i.e., 3155 and 3047 cm^{-1}, are considerably higher than the B3LYP value, 2931 cm^{-1}. For SN stretching vibrations, the B3LYP, MP2, and B97D methods yield (700 cm^{-1}, 972 cm^{-1}), (990 cm^{-1}, 986 cm^{-1}), and (904 cm^{-1}, 877 cm^{-1}), respectively. Comparison with experimental results for C_2-H and SN vibrations noted above suggests that B3LYP yields a better agreement with measurements than MP2 or B97D does. This observation appears to be consistent with other studies.[48−52] Thus, hereafter, we will focus mainly on the results obtained with the B3LYP method.

The B3LYP results for intra- and interionic bond lengths in different ion pair conformations are compiled in Table 2. The distance between the hydrogen atom at the C_2 position of the cation and the hydrogen-bond acceptor atom of the anion for C−H---N interaction is shorter than similar distances for C−H---O and C−H---F interactions. This suggests that the interionic hydrogen-bond interaction of the former is stronger than the latter two (see below).

The cation−anion molecular interactions play a crucial role in the conformer stability. Their interaction strength can be correlated with the weakening of various bonds, such as SN* and SO* of the anion, compared with those in the free anion. Here * denotes explicitly that the atom participates directly in the intermolecular interaction with the cation. A maximum elongation was obtained for the anionic SN* and cationic C_2-H_{24} bonds of **C1** among the same types of bonds in all five conformers. This large bond elongation is attributed to the strong C−H---N cation−anion interaction. In contrast to the SN* elongation in **C1** (and also in **C4**), the SN bonds of **C2**, **C3** and **C5**, which do not participate in molecular interactions, become shortened. Similar changes result also for SO and CF bonds, i.e., elongation for those interacting with, and contraction for those not interacting with, the cation. This state of affairs is in good agreement with other studies, where conformational equilibrium of the Tf_2N anion was examined using Raman spectroscopy (and also density functional calculations).[24,25]

3.2. Molecular Electron Density Topography Analysis.

Here we consider molecular electron density (MED) topography of the ion pair in different conformations. Briefly, Popelier's criteria[53,54] for the existence of X−H···Y type molecular interactions include (a) the existence of a bond critical point (bcp) along a bond path, (b) the proper value of the electron density at the bcp of H···Y, (c) penetration of H and Y atoms, (d) an increase in the net charge of the hydrogen atom, (e) energetic destabilization of hydrogen, (f) decrease of dipolar polarization, and (g) a decrease of hydrogen atomic volume. The topographical properties, in particular, electron density at the bond critical point (ρ_{bcp}), show a linear relationship when correlated with interaction energy and internuclear distances of the complex. Therefore, they offer a useful, quantitative measure to gauge molecular interactions.[55] We mention that the shared electron number employed by Kirchner and others[56−62] in the analysis of the hydrogen-bonded interactions yields a similar linear relationship. It thus provides another useful theoretical tool to study hydrogen bonding interactions in the molecular systems.

The B3LYP results for ρ_{bcp} along a bond path are reported in Table S2 in the Supporting Information for various interactions. The ρ_{bcp} value of the C−H---N (0.03064 au) interaction in **C1** is higher than that of C−H---O and C−H---F interactions in different conformers. This provides another evidence that the C−H---N interaction is stronger than the C−H---O and C−H---F interactions. Comparison of ρ_{bcp} values between ion pair conformers and free ions in Table S2 (Supporting Information) shows that the CH bond participating in C−H---N interactions becomes weakened, whereas the opposite trend is predicted for the methyl and ethyl CH bonds interacting with oxygen atoms of the anion. The latter result is ascribed to the much weaker polar character of alkyl CH groups

dx.doi.org/10.1021/jp502124y | J. Phys. Chem. A 2014, 118, 2547−2557

Table 2. Bond Distances (Å) in Free Cation,[a] Anion,[b] and Different Ion Pair Conformers of 1-Ethyl-3-methylimidazolium Bis(trifluoromethylsulfonyl)imide in the Gas Phase and in the Solution Phase

	C1	S1	C2	S2	C3	S3	C4	S4	C5	S5
	gas	solution	gas	solution	gas	solution	gas	solution	gas	solution
N_1-C_5	1.383	1.384	1.385	1.384	1.383	1.384	1.383	1.385	1.384	1.383
C_5-C_4	1.362	1.363	1.362	1.362	1.362	1.363	1.361	1.363	1.362	1.363
C_4-N_3	1.383	1.385	1.383	1.384	1.383	1.383	1.383	1.384	1.386	1.384
N_3-C_2	1.341	1.338	1.335	1.339	1.340	1.339	1.341	1.336	1.339	1.339
N_3-C_6	1.469	1.465	1.466	1.467	1.469	1.467	1.470	1.465	1.465	1.465
N_1-C_7	1.481	1.477	1.478	1.477	1.481	1.478	1.480	1.476	1.481	1.477
C_7-C_8	1.526	1.526	1.526	1.526	1.526	1.527	1.525	1.527	1.525	1.526
C_5-H_{12}	1.078	1.083	1.078	1.084	1.078	1.083	1.078	1.083	1.078	1.084
C_4-H_{13}	1.078	1.084	1.078	1.083	1.078	1.083	1.078	1.083	1.078	1.084
C_2-H_{14}	1.097	1.080	1.081	1.081	1.086	1.085	1.096	1.078	1.084	1.082
C_6-H_{15}	1.092	1.092	1.091	1.092	1.092	1.092	1.092	1.092	1.092	1.092
C_6-H_{16}	1.092	1.092	1.091	1.092	1.091	1.092	1.092	1.091	1.092	1.092
C_6-H_{17}	1.092	1.089	1.090	1.089	1.090	1.090	1.092	1.088	1.089	1.090
C_7-H_{18}	1.091	1.091	1.091	1.091	1.089	1.091	1.089	1.092	1.090	1.090
C_7-H_{19}	1.094	1.094	1.094	1.094	1.093	1.094	1.094	1.093	1.094	1.093
C_8-H_{20}	1.095	1.094	1.094	1.094	1.095	1.094	1.095	1.094	1.095	1.094
C_8-H_{21}	1.093	1.094	1.094	1.094	1.093	1.094	1.093	1.094	1.093	1.092
C_8-H_{22}	1.091	1.092	1.091	1.092	1.092	1.092	1.091	1.092	1.091	1.093
N−S	1.630*	1.617	1.611	1.615	1.607	1.622*	1.628*	1.614	1.607	1.611
N−S	1.631*	1.621	1.617	1.622	1.617	1.622*	1.628*	1.622	1.617	1.625*
S−C	1.872	1.871	1.866	1.871	1.870	1.871	1.872	1.868	1.869	1.871
S−C	1.874	1.872	1.871	1.872	1.873	1.871	1.872	1.872	1.871	1.876
S−O	1.462	1.467	1.481*	1.468	1.459	1.469	1.461	1.477	1.458	1.475
S−O	1.475*	1.476*	1.485*	1.477*	1.483*	1.472*	1.475*	1.479*	1.482*	1.469*
S−O	1.460	1.468	1.460	1.467	1.460	1.468	1.460	1.474	1.460	1.470
S−O	1.472*	1.474*	1.482*	1.474*	1.484*	1.470*	1.475*	1.470*	1.480*	1.471
C−F	1.332	1.332	1.331	1.331	1.332	1.335	1.335	1.333	1.328	1.334
C−F	1.337	1.335	1.332	1.340	1.338	1.335	1.336	1.333	1.339	1.336
C−F	1.339	1.345	1.339	1.342	1.340	1.337	1.337	1.338	1.358*	1.341*
C−F	1.330	1.333	1.333	1.335	1.327	1.334	1.334	1.336	1.329	1.336
C−F	1.335	1.338	1.338	1.336	1.347	1.335	1.336	1.337	1.343*	1.337*
C−F	1.355*	1.339*	1.339*	1.337*	1.352*	1.342*	1.348*	1.338*	1.347*	1.338*
H_{14}---O		2.234	2.072	2.357	2.179			2.419	1.958	2.213
H_{14}---O		2.432		2.364	2.116			2.479		
H_{14}---N	1.950					2.154	1.976			
H_{14}---F		2.749			2.930					
H_{17}---O	2.104		2.627	2.362	2.153	2.339	2.103	2.560	2.366	
H_{17}---F		2.540		2.922						
H_{18}---O	2.258	2.726	2.531	2.501	2.224	2.521	2.499	2.043	2.490	2.854
H_{18}---F		2.642					2.507		2.674	2.467
H_{21}---F									2.979	
H_{22}---O		2.759	3.304				2.516		2.629	
H_{22}---F	2.545	2.830	2.502	2.770	2.618	2.601		2.575	2.690	
H_{20}---N										2.889
C_2-H_{14}---N angle	173.0						177.0		149.0	
C_2-H_{14}---O angle			151.0		135.0					

*Atom participates in the cation−anion interactions. [a]Free cation (in vacuo): C_5-H_{14} (1.079), C_4-H_{13} (1.079), C_5-H_{12} (1.078), C_6-H_{17} (1.089), C_7-H_{18} (1.092), C_8-H_{21} (1.093). [b]Free anion (in vacuo): S−O (∼1.468), S−N (1.620).

than C_2-H_{14} of the imidazole ring. We also notice that among all conformers, the minimum of ρ_{bcp} for C_2-H_{14} results in the lowest energy **C1** with strong C−H---N interactions.

Weakening of the anionic SN, SO, and CF bonds resulting from interactions with the cation leads to ρ_{bcp} values lower than those of the free anion. An increase of ρ_{bcp} on the other hand was obtained for SO bonds not interacting with the cation compared to those in the free anion. Except for **C1** and **C4**, the SN bonds tend to be stronger in ion pairs than those in the free anion due to the absence of C−H---N interactions.

3.3. Conformer Structures in Solution. It is well-known that solvation exerts a strong influence on molecular systems and modulates their structure, energetics, and reactivity, compared to the case for the gas phase. Therefore, it is important to understand how the surrounding solvent environment affects the molecular interactions in ionic liquids. In the present work we modeled the RTIL environment as a dielectric

dx.doi.org/10.1021/jp502124y | J. Phys. Chem. A 2014, 118, 2547−2557

Table 3. Selected Vibrational Frequencies (cm^{-1}) of Free Cation and Anion and C1, C2, and S1 Conformers of 1-Ethyl-3-methylimidazolium Bis(trifluoromethylsulfonyl)imide Determined with the B3LYP Method[a]

				C1	C2	S1
	EMIm	Tf_2N	experimental	gas phase	gas phase	solution phase
C_4-H_{13}, C_5-H_{12} stretch	3198 (16)		3185 (R), 3165 (IR)			
			3125 (R), 3126 (IR)	3198 (8)	3200 (6)	3110 (61)
C_8-H_{22} stretch			3107 (IR)	3073 (21)	3035 (15)	
C_6-H_{17} stretch	3093 (0)			3072 (65)		
asymm. $H_{18}-C_7-H_{19}$ stretch	3062 (9)			3060 (11)		3039 (15)
asymm. $H_{20}-C_8-H_{21}$ stretch	3042 (1)			3040 (24)		3054 (9)
C_7-H_{19} stretch			2991 (IR)	2991 (33)	2989 (19)	
symm. $H_{15}-C_6-H_{17}$ stretch			2986 (R), 2980 (IR)	2973 (85)	2988 (29)	2986 (11)
asymm $H_{20}-C_8-H_{21}$ stretch			2970 (R), 2958 (IR)	2968 (20)	2969 (16)	
C_2-H_{14} stretch	3202 (30)		2948 (R), 2914 (R)	2931 (735)	3155 (254)	3195 (233)
$N_3-C_4-H_{13}$ rock	1570 (32)		1575 (R), 1574 (IR)	1571 (22)	1574 (34)	1570 (50)
$N_1-C_2-H_{14}$ rock	1562 (54)			1562 (50)	1566 (48)	1562 (19)
$H_{18}-C_7-H_{19}$ scissor	1473 (15)			1480 (9)	1476 (6)	1473 (8)
$H_{15}-C_6-H_{17}$ scissor	1456 (9)		1471 (IR)	1473 (12)	1474 (17)	1470 (16)
$H_{21}-C_8-H_{22}$ scissor	1460 (16)		1458 (R), 1464 (IR)	1466 (11)	1464 (14)	1457 (9)
$H_{15}-C_6-H_{17}$ rock	1448 (16)		1426 (R), 1433 (IR)	1435 (11)	1456 (14)	1422 (15)
					1429 (8)	
CN stretch	1407 (2)			1412 (18)	1317 (13)	
$H_{21}-C_8-H_{22}$ rock	1395 (7)		1390 (IR)	1392 (8)	1396 (9)	1388 (10)
$H_{18}-C_7-H_{19}$ rock	1349 (14)		1340 (R), 1348 (IR)	1350 (8)	1352 (11)	1351 (15)
$N_1-C_2-H_{14}$ rock	1311 (11)		1330 (R), 1331 (IR)	1300 (13)		1320 (12)
SO stretch		1284 (444)	1244 (R)	1295 (585)	1269 (415)	1253 (811)
		1261 (71)	1237 (R)			1235 (142)
$H_{18}-C_7-H_{19}$ twist				1270 (38)	1246 (51)	1247 (27)
$H_{18}-C_7-H_{19}$ twist			1244 (R)	1253 (21)		
CF Stretch		1197 (396)	1227 (IR), 1200 (IR)	1225 (403)	1233 (299)	1196 (241)
		1193 (52)	1182 (IR)	1217 (46)	1214 (225)	1190 (203)
		1186 (92)	1200 (IR), 1182 (IR)	1202 (176)	1211 (179)	1180 (179)
		1182 (167)	1200 (IR), 1182 (IR)	1195 (103)	1197 (177)	1177 (491)
		1175 (160)	1141 (R), 1169 (IR)	1145 (156)	1187 (83)	1167 (142)
			1132 (IR)			
		1169 (307)			1179 (148)	
SC stretch			1169 (IR)	1175 (156)	1168 (134)	
$N_1-C_2-H_{14}$ rock	1148 (108)		1169 (IR)	1170 (98)	1149 (32)	1161 (329)
			1141 (R)			1151 (186)
$H_{21}-C_8-H_{22}$ twist			1092 (R), 1088 (IR)	1078 (64)	1077 (76)	1111 (12)
SO* stretch			1051 (IR)	1070 (127)	1070 (346)	1059 (40)
			1051 (IR) 1038 (IR)	1066 (171)	1038 (237)	1050 (657)
C_7-C_8 stretch			1026 (R), 1022 (R)	1018 (8)	1017 (8)	
$C_2-N_3-C_4$				1006 (12)	1009 (22)	
$N_1-C_2-H_{14}$ wag	805 (38)		963 (R), 960 (IR)	969 (331)		825 (30)
			954 (R), 843 (IR)	946 (231)	902 (32)	
$H_{18}-C_7-H_{19}$ wag			793 (R)	792 (14)	789 (7)	785 (11)
symm CF_3 stretch			754 (R), 752 (IR)	753 (31)		
$C_4-C_5-H_{12}$ wag	729 (21)			724 (33)	716 (29)	
SN stretch			740 (R), 741 (IR)			
		745 (12)	701 (R), 702 (IR)	700 (90)	972 (500)	751 (25)
		695 (23)			700 (16)	692 (39)
CN bond oscillation	642 (15)		650 (IR)	651 (21)	649 (21)	639 (24)
					617 (23)	
SN bond oscillation			592 (R), 569 (R)			
		584 (343)	569 (IR)	587 (308)	633 (111)	562 (522)

[a]Intensities (in KM/mol) are given in parentheses. In the experimental column, R and IR refer to Raman and infrared results.

continuum with $\varepsilon = 38$ and carried out SCRF[31,32] calculations. As mentioned above, this choice of ε value is based on simulation results that imidazolium-based ionic liquids are effectively more polar than acetonitrile.[43−45]

The results for the five lowest energy ion-pair conformations **S1**−**S5** in solution are compared with those in a vacuum, **C1**−**C5**, in Table 1 and in Figure 2. In contrast to the gas-phase results, all three methods, B3LYP, B97D, and MP2, predict that

dx.doi.org/10.1021/jp502124y | J. Phys. Chem. A 2014, 118, 2547−2557

S1 is the lowest energy conformer in solution. As expected, solvation has a significant influence on ion pair conformation and interactions. For example, the C−H---N interaction present in **C1** is completely absent in **S1**. Nonetheless, as in **C1**, the anion in **S1** is in the trans conformation. In general, weakening of cation−anion interactions is predicted in solution, compared to the gas phase. Thus the intramolecular bonds participating in the cation−anion interactions, such as the cationic C_2-H_{14} bond, are shorter and stronger in the solution phase than in the gas phase. The weakening of molecular interactions in the solution phase is also manifested in smaller ρ_{bcp} values for interionic interactions than those in the gas phase (Table S2, Supporting Information). Another interesting result is that the cationic C−H bonds not interacting with the anion are elongated in solution, compared to the gas phase. This bond weakening is attributed to interactions of the cation with the continuum solvent environment.

3.4. Vibrational Analysis. Spectroscopic analysis of the normal vibrations provides useful information about molecular interactions in the system. Specifically, their frequency shifts gauge the strength of molecular interactions involving the bonds under study via vibrational spectroscopy and thus yield microscopic insight into the nature of the interactions.[29,30,58,59] In Table 3 we present B3LYP/6-31G** (scaled by 0.97) derived vibrational frequencies of the lowest energy ion pair conformers in the gas and solution phases, **C1**, **C2**, and **S1**, as well as those of the isolated cation and anion, along with the experimental IR and Raman data in the frequency range 500−3500 cm^{-1}. For additional insight, the experimental spectra are displayed in Figure 3.

We first consider **C1** and **C2**, the two lowest energy complexes in the gas phase in the B3LYP theory. Due to C−H---N interactions in **C1** and C−H---O interactions in **C2**, DFT predicts a substantial downshift of 271 and 47 cm^{-1}, respectively, for the C_2-H_{14} stretching vibration in the ion pair complex with respect to the free cation frequency 3202 cm^{-1}. We note that a large red shift of this mode was also found in [EMIm] paired with other anions, such as acetate and ethyl sulfate.[29,30] The C_2 position is very often considered the predominant site for both interionic and intermolecular interactions.[60] The significant red shift of the C_2-H_{24} stretching mode we found with DFT and the absence of peaks at around 3200 cm^{-1} in the experimental spectra lend support to this view.

Strong cation−anion interactions in **C1** are also manifested in the appearance of intense triplet vibrations in the frequency range 2968−2991 cm^{-1}. A similar triplet is observed in the IR spectrum in essentially the same range, 2958−2991 cm^{-1}. Upon ion pairing, the $H_{15}-C_6-H_{17}$ rock vibration of the free cation at 1448 cm^{-1} shifts down to 1435 cm^{-1}. This correlates well with the 1426/1433 cm^{-1} (Raman/IR) peaks in the experimental spectra. Contraction of CN bonds in **C1** results in a small blue shift of their stretching mode to 1412 cm^{-1} with respect to 1407 cm^{-1} of the free cation. For stretching vibrations of the anion SO* bonds that participate in the interactions with the cation, we obtained 1070 cm^{-1} and 1066 cm^{-1} in **C1** and 1070 cm^{-1} and 1038 cm^{-1} in **C2**, resulting in a red shift of 214−218 cm^{-1} in **C1** and 214−246 cm^{-1} in **C2** with respect to its free anion value 1284 cm^{-1}. It is interesting that DFT predictions for the SO* stretching frequencies for **C2** are in better agreement with experiments than those for **C1**; the latter are somewhat higher than the experimental results. One potential reason for this is that the actual interactions involving SO* groups of **C1** in a real RTIL are stronger than those in an isolated ion pair. Another possibility is the presence of a considerable population of **C2** that contributes to the experimental spectra. Because the energy difference between **C1** and **C2** is less than the thermal energy in the B3LYP theory as noted above, the contribution from **C2** could be indeed significant. In contrast to SO*, similar vibrations of SO and CF bonds that do not interact with the cation show a blue shift of 11 and 13−28 cm^{-1} compared to their free anion frequencies, 1284 and 1182−1197 cm^{-1}, respectively. The results for CF stretching vibrations are in good agreement with the measurements (cf. Table 3). An intense $N_1-C_2-H_{14}$ rock vibration of the free cation at 1148 cm^{-1} shifts to 1170 cm^{-1} in **C1**, in concert with the IR peak at 1169 cm^{-1}. Another intense mode at 1078 cm^{-1} assigned to the HCH twist of the ion pair complex can be correlated to the experimentally observed signals at 1092/1088 cm^{-1}.

To understand the solvation effect on vibrational spectra and to gain insight into how well the SCRF method captures the solvation effect in RTILs, we compare B3LYP results for vibrational spectra of **C1** and **S1**. C_4-H_{13} and C_5-H_{12} stretching vibrations of **S1** show a red shift of 88 cm^{-1} with respect to 3198 cm^{-1} of the isolated cation and the **C1** complex (Table 3). This seems to confirm the aforementioned involvement of hydrogen atoms of C_4/C_5 in interactions with the solution environment. Another pronounced feature is that compared to the free cation, the C_2-H_{14} stretching mode of **S1** does not show any significant red shift in striking contrast to that of **C1**. This lends support to the view that the interionic interactions are weakened considerably by nonspecific solvation. Further evidence for the weakened interactions in solution is the SO and CF stretching vibrations of the anion in **S1**, which are very close in frequency to those of the free anion. A similar behavior is noted for SN stretching vibrations, which exhibit a nearly negligible shift in solution whereas a red shift of 45 cm^{-1} is obtained in the gas phase, compared to results for the free anion.

We pause here for perspective. Our analysis above shows clearly that ion pair interactions and their structural and vibrational properties are modulated significantly by their interactions with the environment. This implies that in principle, inclusion of solvation effects would be needed for proper understanding of RTIL properties, such as C_2-H_{14} and SO stretching vibrations, accessible via various vibrational spectroscopies. Because of their high intensity as well as good correlation of their frequency shifts with the interaction strength as analyzed above, these vibrations can serve as an ideal probe to measure interionic interactions. To our surprise, the present analysis of these modes and others appears to indicate that the DFT results of the ion pair in the gas phase capture liquid-phase vibrational spectroscopy measurements better than those in the solution phase do. This counterintuitive finding is ascribed mainly to overestimation of solvation influence in the SCRF approach couched in the dielectric continuum description; i.e., a continuum solvent is more polar than an actual molecular solvent. We note that this overestimation is well appreciated in connection with normal polar solvents.[61] We thus speculate that solvation-induced weakening of interionic hydrogen bonds compared to the isolated ion pair is overestimated in the dielectric continuum description and as a consequence, their stretching frequencies determined via SCRF calculations are considerably higher than the actual frequencies in the real molecular solvent environment.

Returning to our main thread, we obtain further insight into the frequency shifts by calculating the difference electron density coupled with electron density topography. Recently, Joseph[62] et al. have studied frequency shifts of different types of hydrogen bonds. These authors point out that a variation of the X−H bond distance in a X−H----Y hydrogen bond type is influenced by the polarity of the X−H bond. Highly polar X−H bonds such as O−H, N−H, and F−H show bond elongation and red shifts compared to the case of the free state, whereas less polar X−H bonds, e.g., C−H, result in bond contraction and blue shifts, in excellent agreement with our results above. Bond contraction is due to electron affinity of X causing a net gain of electron density at the X−H bond region in the presence of Y. Here we have used difference electron density to analyze the reorganization of electron density caused by hydrogen-bonded interactions. The difference electron density, $\Delta\rho$, was determined by subtracting the sum of electron densities of the individual anion and cation from the corresponding electron density of the complex.

Figures 4 and 5 display $\Delta\rho$ maps for the lowest energy conformers determined with the B3LYP method in the gas and solution phases, respectively. To explain frequency shifts of characteristic vibrations of the cation and anion, we derive the difference electron density contours in different planes, viz., a plane passing through oxygen atoms of the anion participating in the anion−cation interactions (Figure 4) and a plane passing through the imidazole ring (Figure 5) (data are summarized in Table 4). The blue and red lines denote, respectively, positively and negatively valued $\Delta\rho$, where the contours in the range of ±0.001 to ±0.0009 au are shown explicitly. For S−O bonds participating in the C−H···O interactions, the bond critical points are located in the red regions where electron density is depleted. This result demonstrates that the red shifts in their frequencies are caused by bond weakening (Figure 4). In contrast, the bond critical points of the S−O and C−F bonds not interacting with the cation are situated in the blue regions of enhanced electron density, indicating bond strengthening. In solution, the bond critical points of the cationic C−H bonds not interacting with the anion are located in the red regions (Figure 5). This finding further supports our view above that

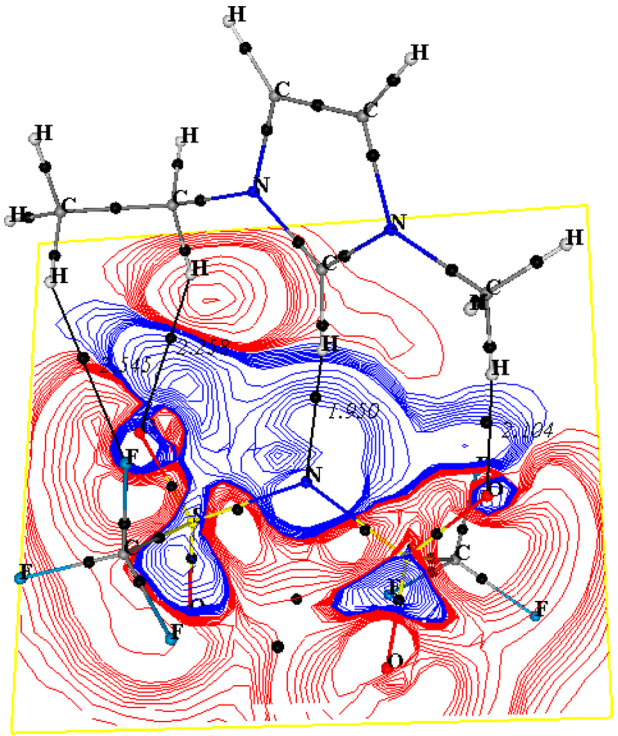

Figure 4. Difference electron density maps for the **C1** conformer in the gas phase. Contours in the range from ±0.001 to ±0.0009 au are shown. Filled circles in black represent the bond critical points. See text for details.

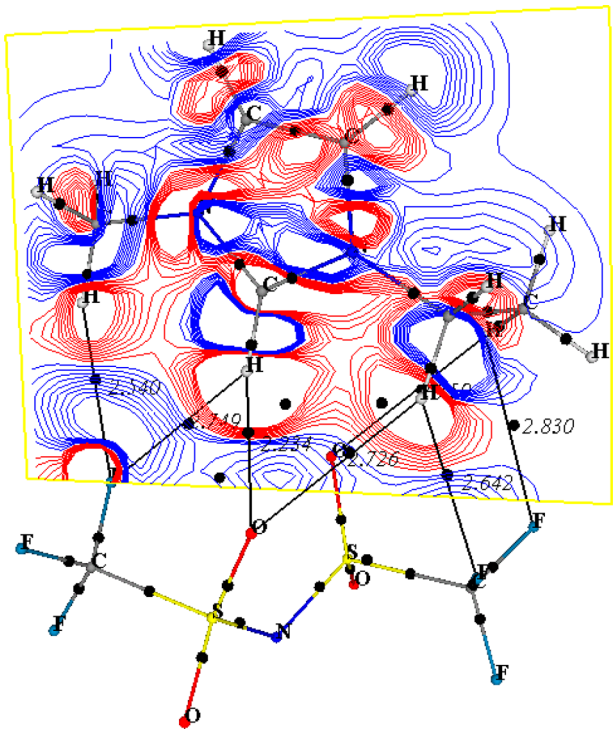

Figure 5. Difference electron density maps for the **S1** conformer in solution. Details are the same as in Figure 4.

Table 4. Difference Electron Density at BCP of Different Bonds in C1 and S1 Conformer

	C1	S1
	gas phase	solution phase
C_2-H_{14}	−0.0076	0.00258
C_4-H_{13}	−0.0010	−0.00281
C_5-H_{12}	−0.0011	−0.0028
C_6-H_{17}	0.00283	0.00069
C_7-H_{18}	0.00434	0.00226
C_8-H_{22}	0.00222	0.00118
N−S	−0.00412	0.0007
N−S	−0.00433	−0.00102
S−C	0.00095	0.00214
S−C	0.0000	0.00176
S−O	0.00282	−0.00464
S−O	−0.00384	0.0004
S−O	0.00349	−0.00372
S−O	−0.00201	0.00016
C−F	0.00666	0.00565
C−F	0.00541	0.00544
C−F	−0.00425	0.00142
C−F	0.00585	0.00456
C−F	0.00471	0.00397
C−F	0.00593	0.00548

dx.doi.org/10.1021/jp502124y | J. Phys. Chem. A 2014, 118, 2547−2557

electron density of C−H bonds decreases due to their interactions with the solvent environment. This leads to an increase of their bond length and red shifts of their vibrational frequency compared to the case of free cation and the ion pair in the gas phase.

4. CONCLUDING REMARKS

In this paper we presented a systematic analysis of the electronic structure and molecular interactions in the room-temperature ionic liquid 1-ethyl-3-methylimidazolium bis-(trifluoromethylsulfonyl)imide employing the density functional and MP2 methods as well as experimental vibrational spectroscopy. Different ion pair conformations were simulated on the basis of different possible interactions between the cation and anion in both the gas and solution phases. The SCRF approach based on the dielectric continuum solvent description was employed for electronic structure calculations in the latter phase. As far as vibrational frequencies are concerned, we found that the B3LYP method generally yields a better agreement with experiments than MP2 or B97D, consistent with other existing studies.

It was found that cation−anion interactions within the ion pair and its interactions with the surrounding media exert a strong influence on its structure and vibrational spectra through reorganization of its electron density. In both the gas and solution phases, B3LYP calculations predict that the anion in the lowest energy ion pair state adopts a trans conformation in accordance with measurements. Nevertheless, a significant presence of cis conformers is also expected because the energy difference between the trans and cis conformers is comparable to a thermal energy.

In the gas phase, the lowest energy conformer exhibits a characteristically strong C_2−H_{14}---N interaction, accompanied by a substantial red shift of C_2−H_{14} stretching vibrational frequency, according to B3LYP calculations. Contractions of SO and CF moieties, which do not participate in interionic interactions, on the other hand, result in blue shifts of their stretching vibrations relative to those of the free anion. In contrast, in the dielectric continuum solvent, a red shift is predicted for these vibrations due to ion−solvent interactions. Surprisingly, the DFT results in the gas phase show a better agreement with IR and Raman spectroscopy measurements than those in the solution phase do. This was ascribed to the overestimation of solvation effects in the dielectric continuum description.

Our present and previous studies suggest that a combined effort of computational and experimental methods provide a powerful approach to analyze and understand molecular structures and interactions: (1) the computational analysis allows experimental signals to be properly assigned to vibrational modes and (2) the experimental data enables the identification of the most likely configurations from different possibilities obtained from computations. Nevertheless, in view of the counterintuitive dielectric continuum results obtained in the present work, it would be very worthwhile in the future to extend the present approach to describe the ionic liquid environment in an explicit molecular representation and study its influence. This would yield most detailed molecular insight into ion pair interactions and structure in room-temperature ionic liquids.

■ ASSOCIATED CONTENT

Supporting Information

Vibrational frequencies of the lowest energy ion-pair complex of 1-ethyl-3-methylimidazolium bis(trifluoromethylsulfonyl)-imide in the B3LYP, B97D, and MP2 frameworks and B3LYP results for electron density at BCPs of five lowest energy ion-pair conformations in the gas and solution phase. This material is available free of charge via the Internet at http://pubs.acs.org.

■ AUTHOR INFORMATION

Corresponding Author

*Permanent address: Carnegie Mellon University.

Present Address

[¶]Technische Thermodynamik, Universtät Bremen, Germany.

Notes

The authors declare no competing financial interest.

■ ACKNOWLEDGMENTS

This work was supported in part by NSF Grant No. CHE-1223988 and by EPSRC Grant No. EP/K00090X/1. K.N. and J.K. gratefully acknowledge support from the German Research Foundation and the Erlangen Graduate School in Advanced Optical Technologies (SAOT).

■ REFERENCES

(1) Welton, T. Room-Temperature Ionic Liquids. Solvents for Synthesis and Catalysis. *Chem. Rev.* **1999**, *99*, 2071−2083.

(2) Wasserscheid, P.; Keim, W. Ionic Liquids-New "Solutions" for Transition Metal Catalysis. *Angew. Chem., Int. Ed.* **2000**, *39* (21), 3772−3789.

(3) Seddon, K. R. Ionic Liquids for Clean Technology. *J. Chem. Technol. Biotechnol.* **1997**, *68*, 351−356.

(4) Hagiwara, R.; Ito, Y. Room temperature ionic liquids of alkylimidazolium cations and fluoroanions. *J. Fluorine Chem.* **2000**, *105*, 221−227.

(5) Huddleston, J. G.; Willauer, H. W.; Swatloski, R. P.; Visser, A. E.; Rogers, R. D. Room temperature ionic liquids as novel media for 'clean' liquid−liquid extraction. *Chem. Common.* **1998**, 1765−1766.

(6) Broker, G. A.; Rogers, R. D. Characterization and comparison of hydrophilic and hydrophobic room temperature incorporating the imidazolium cation. *Green Chem.* **2001**, *3*, 156−164.

(7) Garcia, B.; Lavallee, S.; Perron, G.; Michot, C.; Armand, M. Room temperature molten salts as lithium battery electrolyte. *Electrochim. Acta* **2004**, *49*, 4583−4588.

(8) Every, H. A.; Bishop, A. G.; MacFarlane, D. R.; Oradd, G.; Forsyth, M. Transport properties in a family of dialkylimidazolium ionic liquids. *Phys. Chem. Chem. Phys.* **2004**, *6*, 1758−1765.

(9) Bonhote, P.; Dias, A.; Papageorgiou, N.; Kalyanasundaram, K.; Gratzel, M. Hydrophobic, Highly Conductive Ambient-Temperature Molten Salts. *Inorg. Chem.* **1996**, *35*, 1168−1178.

(10) Koch, V. R.; Nanjundah, C.; Appetecchi, G. B.; Scrosati, B. The Interfacial Stability of Li with Two New Solvent-Free Ionic Liquids: 1,2-Dimethyl-3-propylimidazolium Imide and Methide. *J. Electrochem. Soc.* **1995**, *142*, L116−L118.

(11) Gejji, S. P.; Suresh, C. H.; Babu, K.; Gadre, S. R. *Ab Initio* Structure and Vibrational Frequencies of $(CF_3SO_2)^-{}_2NLi^+$ Ion Pairs. *J. Phys. Chem. A* **1999**, *103* (37), 7474−7480.

(12) Holbrey, J. D.; Matthew Reichert, W.; Rogers, R. D. Crystal structures of imidazolium bis(trifluoromethanesulfonyl)imide 'ionic liquid' salts: the first organic salt with a cis-TFSI anion conformation. *Dalton Trans.* **2004**, 2267−2271.

(13) Noack, K.; Schulz, P. S.; Paape, N.; Kiefer, J.; Wasserscheid, P.; Leipertz, A. The role of the C2 position in interionic interactions of

imidazolium based ionic liquids: a vibrational and NMR spectroscopic study. *Phys. Chem. Chem. Phys.* **2010**, *12*, 14153−14161.
(14) Hunt, P. A. Why Does a Reduction in Hydrogen Bonding Lead to an Increase in Viscosity for the 1-Butyl-2,3-dimethyl-imidazolium-Based Ionic Liquids? *J. Phys. Chem. B* **2007**, *111*, 4844−4853.
(15) Hunt, P. A.; Gould, I. R.; Kirchner, B. The Structure of Imidazolium-Based Ionic Liquids: Insights From Ion-Pair Interactions. *Aust. J. Chem.* **2007**, *60*, 9−14.
(16) Fumino, K.; Peppel, T.; Geppert-Rybczynska, M.; Zaitsau, D. H.; Lehmann, J. K.; Verevkin, S. P.; Kockerling, M.; Ludwig, R. The influence of hydrogen bonding on the physical properties of ionic liquids. *Phys. Chem. Chem. Phys.* **2011**, *13*, 14064−14075.
(17) Fumino, K.; Wulf, A.; Ludwig, R. Strong, Localized, and Directional Hydrogen Bonds Fluidize Ionic Liquids. *Angew. Chem., Int. Ed.* **2008**, *47*, 8731−8734.
(18) Peppel, T.; Roth, C.; Fumino, K.; Paschek, D.; Kockerling, M.; Ludwig, R. The Influence of Hydrogen-Bond Defects on the Properties of Ionic Liquids. *Angew. Chem., Int. Ed.* **2011**, *50*, 6661−6665.
(19) Lehmann, S. B. C.; Roatsch, M.; Schöppke, M.; Kirchner, B. On the physical origin of the cation−anion intermediate bond in ionic liquids Part I. Placing a (weak) hydrogen bond between two charges. *Phys. Chem. Chem.. Phys.* **2010**, *12*, 7473−7486.
(20) Brehm, M.; Weber, H.; Pensado, A. S.; Stark, A.; Kirchner, B. Proton transfer and polarity changes in ionic liquid−water mixtures: a perspective on hydrogen bonds from ab initio molecular dynamics at the example of 1-ethyl-3-methylimidazolium acetate−water mixtures—Part 1. *Phys. Chem. Chem. Phys.* **2012**, *14*, 5030−5044.
(21) Pensado, A. S.; Brehm, M.; Thar, J.; Seitsonen, A. P.; Kichner, B. Effect of Dispersion on the Structure and Dynamics of the Ionic Liquid 1-Ethyl-3-methylimidazolium Thiocyanate. *ChemPhysChem.* **2012**, *13*, 1845−1853.
(22) Malberg, F.; Pensado, A. S.; Kirchner, B. The bulk and the gas phase of 1-ethyl-3-methylimidazolium ethylsulfate: dispersion interaction makes the difference. *Phys. Chem. Chem. Phys.* **2012**, *14*, 12079−12082.
(23) Berg, R. W.; Deetlefs, M.; Seddon, K. R.; Shim, I.; Thompson, J. M. Raman and ab Initio Studies of Simple and Binary 1-Alkyl-3-methylimidazolium Ionic Liquids. *J. Phys. Chem. B* **2005**, *109*, 19018−19025.
(24) Umebayashi, Y.; Fujimori, T.; Sukizaki, T.; Asada, M.; Fujii, K.; Kanazaki, R.; Ishiguro, S. Evidence of Conformational Equilibrium of 1-Ethyl-3-methylimidazolium in Its Ionic Liquid Salts: Raman Spectroscopic Study and Quantum Chemical Calculations. *J. Phys. Chem. A* **2005**, *109*, 8976−8982.
(25) Fujii, K.; Fujimori, T.; Takamuku, T.; Kanzaki, R.; Umebayashi, Y.; Ishiguro, S. Conformational Equilibrium of Bis-(trifluoromethanesulfonyl) Imide Anion of a Room-Temperature Ionic Liquid: Raman Spectroscopic Study and DFT Calculations. *J. Phys. Chem. B* **2006**, *110*, 8179.
(26) Lassègues, J. C.; Grondin, J.; Holomb, R.; Johansson, P. Raman and ab initio study of the conformational isomerism in the 1-ethyl-3-methyl-imidazolium bis(trifluoromethanesulfonyl)imide ionic liquid. *J. Raman Spectrosc.* **2007**, *38*, 551−558.
(27) Köddermann, T.; Wertz, C.; Heintz, A.; Ludwig, R. Ion-Pair Formation in the Ionic Liquid 1-Ethyl-3-methylimidazolium Bis-(triflyl)imide as a Function of Temperature and Concentration. *ChemPhysChem* **2006**, *7*, 1944−1949.
(28) Tsuzuki, S.; Tokuda, H.; Hayamizu, K.; Watanabe, M. Magnitude and Directionality of Interaction in Ion Pairs of Ionic Liquids: Relationship with Ionic Conductivity. *J. Phys. Chem. B* **2005**, *109*, 16474−16481.
(29) Dhumal, N. R.; Kiefer, J.; Kim, H. J. Molecular Interactions in 1-Ethyl-3-methylimidazolium Acetate Ion Pair: A Density Functional Study. *J. Phys. Chem. A* **2009**, *113*, 10397−10404.
(30) Dhumal, N. R.; Kim, H. J.; Kiefer, J. Electronic Structure and Normal Vibrations of the 1-Ethyl-3-methylimidazolium Ethyl Sulfate Ion Pair. *J. Phys. Chem. A* **2011**, *115*, 3551−3558.
(31) Tomasi, J.; Persico, M. Molecular Interactions in Solution: An Overview of Methods Based on Continuous Distributions of the Solvent. *Chem. Rev.* **1994**, *94*, 2027−2094.
(32) Cramer, C. J.; Truhlar, D. Implicit Solvation Models: Equilibria, Structure, Spectra, and Dynamics. *Chem. Rev.* **1999**, *99*, 2161−2200.
(33) For an extensive list of references on experimental and computational study of effective polarity of ionic liquids, see: Shim, Y.; Kim, H. J. Free Energy and Dynamics of Electron-Transfer Reactions in a Room Temperature Ionic Liquid. *J. Phys. Chem. B* **2007**, *111*, 4510−4519.
(34) Frisch, M. J.; et al. *Gaussian 03*, Revision D.01; Gaussian, Inc.: Wallingford, CT, 2004.
(35) Becke, A. D. Density-functional thermochemistry. III. The role of exact exchange. *J. Chem. Phys.* **1993**, *98*, 5648−5652.
(36) Lee, C.; Yang, W.; Parr, R. G. Development of the Colle-Salvetti correlation-energy formula into a functional of the electron density. *Phys. Rev. B* **1988**, *37*, 785−789.
(37) Grimme, S. Semiempirical GGA-type density functional constructed with a long-range dispersion correction. *J. Comput. Chem.* **2006**, *27*, 1787−1799.
(38) Limaye, A. C.; Gadre, S. R. UNIVIS-2000: An indigenously developed comprehensive visualization package. *Curr. Sci. (India)* **2001**, *80*, 1296−1301.
(39) Balanarayan, P.; Gadre, S. R. Topography of molecular scalar fields. I. Algorithm and Poincaré−Hopf relation. *J. Chem. Phys.* **2003**, *119*, 5037−5043.
(40) Jeon, J.; Kim, H. J. Free Energies of Electron Transfer Reactions in Polarizable, Nondipolar, Quadrupolar Solvents. *J. Phys. Chem. A* **2000**, *104*, 9812−9815.
(41) Jeon, J.; Kim, H. J. A Continuum Reaction Field Theory of Polarizable, Nondipolar, Quadrupolar Solvents: Ab Initio Study of Equilibrium Solvation in Benzene. *J. Solution Chem.* **2001**, *30*, 849−860.
(42) Jeon, J.; Kim, H. J. A continuum theory of solvation in quadrupolar solvents. II. Solvation free energetics, dynamics, and solvatochromism. *J. Chem. Phys.* **2003**, *119*, 8626−8635.
(43) Shim, Y.; Choi, M. Y.; Kim, H. J. A molecular dynamics computer simulation study of room-temperature ionic liquids. I. Equilibrium solvation structure and free energetics. *J. Chem. Phys.* **2005**, *122*, 044510.
(44) Shim, Y.; Jeong, D.; Manjari, S.; Choi, M. Y.; Kim, H. J. Solvation, Solute Rotation and Vibration Relaxation, and Electron-Transfer Reactions in Room-Temperature Ionic Liquids. *Acc. Chem. Res.* **2007**, *40*, 1130−1137.
(45) Shim, Y.; Kim, H. J. Dielectric Relaxation and Solvation Dynamics in a Room-Temperature Ionic Liquid: Temperature Dependence. *J. Phys. Chem. B* **2013**, *117*, 11743−11752.
(46) Kiefer, J.; Fries, J.; Leipertz, A. Experimental Vibrational Study of Imidazolium-Based Ionic Liquids: Raman and Infrared Spectra of 1-Ethyl-3-methylimidazolium Bis(trifluoromethylsulfonyl)imide and 1-Ethyl-3-methylimidazolium Ethylsulfate. *Appl. Spectrosc.* **2007**, *61*, 1306−1311.
(47) Noack, K.; Schulz, P. S.; Paape, N.; Kiefer, J.; Wasserscheid, P.; Leipertz, A. The role of the C2 position in interionic interactions of imidazolium based ionic liquids: a vibrational and NMR spectroscopic study. *Phys. Chem. Chem. Phys.* **2010**, *12*, 14153−14161.
(48) Skarmoutsos, I.; Dellis, D.; Matthews, R. P.; Welton, T.; Hunt, P. A. Hydrogen Bonding in 1-Butyl- and 1-Ethyl-3-methylimidazolium Chloride Ionic Liquids. *J. Phys. Chem. B* **2012**, *116*, 4921−4933.
(49) Yadava, U.; Singh, M.; Roychoudhury, M. Gas-phase conformational and intramolecular $\pi-\pi$ interaction studies on some pyrazolo-[3,4-d]pyrimidine derivatives. *Comput. Theor. Chem.* **2011**, *977*, 134−139.
(50) Šebestík, J.; Šafařík, M.; Bouř, P. Ferric Complexes of 3-Hydroxy-4-pyridinones Characterized by Density Functional Theory and Raman and UV−vis Spectroscopies. *Inorg. Chem.* **2012**, *51*, 4473−4481.
(51) Rondino, F.; Paladini, A.; Ciavardini, A.; Casavola, A.; Catone, D.; Satta, M.; Barth, H.; Giardini, A.; Speranza, M.; Piccirillo, S. Chiral

recognition between 1-(4-zluorophenyl)ethanol and 2-butanol: higher binding energy of homochiral complexes in the gas phase. *Phys. Chem. Chem. Phys.* **2011**, *13*, 818−824.
(52) Burgueño-Tapia, E.; Cerda-García-Rojas, C. M.; Joseph-Nathan, P. Conformational analysis of perezone and dihydroperezone using vibrational circular dichroism. *Phytochemistry* **2012**, *74*, 190−195.
(53) Kock, U.; Popelier, P.L. A. Characterization of C-H-O Hydrogen Bonds on the Basis of the Charge Density. *J. Phys Chem. A* **1995**, *99*, 9747−9754.
(54) Popelier, P. L. A. Characterization of a Dihydrogen Bond on the Basis of the Electron Density. *J. Phys. Chem. A.* **1998**, *102*, 1873−1878.
(55) Bader, R. F. W. *Atoms in Molecules: A Quantum Theory*; Clarendon: Oxford, U.K., 1990.
(56) Wendler, K.; Thar, J.; Zahn, S.; Kirchner, B. Estimating the Hydrogen Bond Energy. *J. Phys. Chem. A* **2010**, *114*, 9529−9536.
(57) Thar, J.; Kirchner, B. Hydrogen Bond Detection. *J. Phys. Chem. A* **2006**, *110*, 4229−4237.
(58) Lasségues, J. C.; Grondin, J.; Holomb, R.; Johansson, P. Raman and ab initio study of the conformational isomerism in the 1-ethyl-3-methyl-imidazolium bis(trifluoromethanesulfonyl)imide ionic liquid. *J. Raman Spectrosc.* **2007**, *38*, 551−558.
(59) Lasségues, J.-C.; Grondin, J.; Cavagnat, D.; Johansson, P. New Interpretation of the CH Stretching Vibrations in Imidazolium-Based Ionic Liquids. *J. Phys. Chem. A* **2009**, *113*, 6419−6421.
(60) Kempter, V.; Kirchner, B. The role of hydrogen atoms in interactions involving imidazolium-based ionic liquids. *J. Mol. Struct.* **2010**, *972*, 22−34.
(61) Morita, T.; Ladanyi, B. M.; Hynes, J. T. Polar solvent contributions to activation parameters for model ionic reactions. *J. Phys. Chem.* **1989**, *93*, 1386−1392.
(62) Joseph, J.; Jemmis, E. D. Red-, Blue-, or No-Shift in Hydrogen Bonds: A Unified Explanation. *J. Am. Chem. Soc.* **2007**, *129*, 4620−4632.